

Minimal decomposition entropy and optimal representations of absolutely maximally entangled states

N Ramadas ^{1,2,*}

¹*Center for Quantum Information, Communication, and Computation,
Indian Institute of Technology Madras, Chennai 600036, India*

²*Division of Sciences, Krea University, Sri City 517646, India.*[†]

Understanding and classifying multipartite entanglement is fundamental to quantum information processing. A useful measure of multipartite entanglement is the minimal decomposition entropy, defined as the minimum of the Rényi entropy S_q associated with the state's decomposition over all local product bases. This quantity identifies the product bases in which the state is maximally localized, thereby yielding optimal representations for analyzing local-unitary equivalence and structural properties of multipartite states.

We investigate the minimal decomposition entropy for absolutely maximally entangled (AME) states, a class of highly entangled states characterized by their maximal entanglement across any bipartitions. We present a numerical algorithm for computing the minimal decomposition entropy for finite $q > 1$. Entropy distributions for AME and Haar-random states are obtained for $q = 2$ and $q = \infty$ in qubit, qutrit, and ququad systems. For $q = 2$, AME states of four qutrits and four ququads exhibit smaller minimal decomposition entropy than Haar-random states, indicating more localized optimal representations. For $q = \infty$, corresponding to the geometric measure of entanglement, AME states display higher entanglement than Haar-random states. The algorithm additionally produces simpler and sparser decompositions of known AME states, aiding in distinguishing genuinely quantum AME states from those associated with classical combinatorial designs.

I. INTRODUCTION

Non-classical correlations in many-body systems play a crucial role in various physical phenomena, which are important for applications in quantum computing, information processing, and communication. Among these, quantum entanglement is a particularly important non-classical correlation, making its understanding and classification vital. Quantum entanglement in pure states is well understood in the case of bipartite systems. However, in systems involving more than two parties, the entanglement can be distributed various ways, making its characterization a more challenging problem. For example, in a three-qubit system, the GHZ state has genuine tripartite entanglement, while the W-state has zero tripartite entanglement. On the other hand, the W-state maximizes the total bipartite entanglement shared among all pairs of qubits. At an application level, the W-state is more robust to qubit loss compared to the GHZ state [1].

Several measures have been proposed to quantify pure multipartite entanglement. In this work, we focus on the minimal decomposition entropy introduced by Enríquez *et al.*, also known as the minimal Rényi-Ingarden-Urbanik entropy [2]. The decomposition entropy quantifies the entropy of the probability distribution associated with the coefficients of a quantum state in a given orthonormal basis. When the Rényi entropy is used, this leads to the Rényi-Ingarden-Urbanik entropy,

S_q , defined for $q \geq 0$. The minimal decomposition entropy is obtained by minimizing S_q over all product bases, thereby providing a measure of entanglement for each value of q .

In this work, we use the minimal decomposition entropy to investigate a class of multipartite states known as absolutely maximally entangled (AME) states [3]. The defining feature of AME states is their maximal entanglement across all bipartitions, a property that enables their application in various quantum information tasks. AME states serve as a resource in quantum parallel transportation and secret sharing schemes [3]. They are related to classical error correcting codes [4, 5] and quantum error correcting codes [6–9]. In holography theories and high energy physics, AME states are referred to as perfect tensors [10], and they enable the construction of simplified models of the AdS/CFT correspondence—most notably the “HaPPY” quantum error-correcting code [10–16].

The existence of AME states of N qudits, denoted as $\text{AME}(N, d)$, remains open problem in general, and is listed as Problem 35 in a list of open problems in quantum information [17]. It is established that qubit AME states exist only for $N = 2, 3, 5$, and 6 [6, 18–20]. AME states exist for any number of parties, provided the local dimension is sufficiently large [5]. A table maintained online provides known constructions of AME states [21]. AME states are constructed from graph states [22, 23] classical maximum distance separable codes [5, 24], and classical combinatorial designs such as orthogonal Latin squares and orthogonal arrays [25–27].

The use of minimal decomposition entropy to characterize AME states offers several potential advantages. It can, for instance, be used to classify AME states based on their interconvertibility using local unitary

* ramadas.nedivarambath@krea.edu.in

[†] Present address

(LU) transformations. Two N -party pure states, $|\Psi\rangle$ and $|\Psi'\rangle$, are said to be LU equivalent if there exists a set of local unitary operators u_1, u_2, \dots, u_N such that $|\Psi'\rangle = (u_1 \otimes u_2 \otimes \dots \otimes u_N) |\Psi\rangle$. LU-equivalent states have identical entanglement content, making them equally useful for any application. Allowing local operations along with classical communication leads to a broader classification under the Local Operations and Classical Communication (LOCC) scheme [28, 29], in which the entanglement content of a state cannot increase, providing a partial ordering of states based on convertibility. A coarser classification is provided by stochastic LOCC (SLOCC) [1, 30], which considers conversions achievable with a nonzero probability of success. For AME states, however, the LU, LOCC, and SLOCC classes coincide, so it suffices to consider only LU equivalence in their classification [31].

The minimal decomposition entropy is also useful for identifying an optimal representation of an AME state within its equivalence class. The decomposition entropy S_q measures the localization of a quantum state in a given orthonormal basis, and is also referred to as participation entropy [32]. By minimizing the decomposition entropy, product bases in which the state is least delocalized can be identified, thereby providing an optimal representation of the state within its LU equivalence class. Since the measure becomes increasingly sensitive to localization for larger values of q , lower values of q are typically preferred.

An optimal representation can provide a simpler and sparser form of the state, facilitating the investigation of key properties such as structure and symmetries. This is particularly useful for analyzing numerically generated states. In cases where no known construction methods are available, numerical algorithms are employed to generate AME states. A notable example is the first discovery of an AME(4, 6) state, which was obtained numerically [33]. However, such numerically derived states often exhibit full support in the computational basis, making them difficult to analyze both algebraically and structurally. In this context, finding a sparse representation of the state is highly advantageous. Additionally, an optimal representation can offer insights into whether the state is LU-equivalent to a known construction or represents a novel class of AME states. Sparse states also help reduce computational resources, such as memory and processing time, if they are to be used in classical simulation and computation.

An optimal representation is also valuable for determining whether a given AME state is *genuinely quantum*. An AME state is considered genuinely quantum if it cannot be constructed from a classical combinatorial design [34]. For instance, AME states of four parties can be constructed from combinatorial designs known as orthogonal Latin squares for all local dimensions $d \geq 3$, except for $d = 6$. The existence of orthogonal Latin squares of order 6, famously known as ‘‘Euler’s 36 officers problem,’’ admits no classical solution [35]. However,

quantum solutions to the problem, given by AME(4, 6) states, have been found [33, 36–39], and these are considered genuinely quantum. In this context, an optimal representation of the AME state is crucial for analyzing its structure and determining whether it is genuinely quantum.

Finding the minimal decomposition entropy in the case of multipartite states is challenging due to lack of known analytical techniques. Therefore, numerical methods are employed. In [40], a random walk method is used to find the minimal decomposition entropy. In the present work, we propose a new algorithm for finding minimal decomposition entropy for finite $q > 1$ based on the complex L_p -norm principal component analysis, wherein a local optimization is performed in each step that involves gradient ascent. Hence, it is efficient and converges faster compared to the random walk method. However, the algorithm cannot be used for cases $q \leq 1$ as the gradient may not exist due to non-differentiability at certain points, such as zero.

In this work, we analyze the minimal decomposition entropy of AME states and compare it to that of Haar-random states. A lower bound for the minimal decomposition entropy is established for AME states. The distributions of decomposition entropy and its minimal value for $q = 2$ and $q = \infty$ are computed for AME and Haar-random states in qubit, qutrit, and ququad systems with varying numbers of parties. For $q = 2$, it is observed that AME states of four qutrits and four ququads have smaller minimal decomposition entropy compared to Haar-random states, suggesting that they can be more optimally represented. For $q = \infty$, which is related to the geometric measure of entanglement, AME states are found to be highly entangled in terms of minimal decomposition entropy or the geometric measure of entanglement, in contrast to Haar-random states. We also identify new states that exhibit the maximum minimal decomposition entropy for both $q = 2$ and $q = \infty$. Additionally, we demonstrate the use of the algorithm to obtain simpler and sparser representations of AME states, and discuss its usefulness in determining whether a given AME state is genuinely quantum or can be constructed from classical combinatorial designs.

II. ABSOLUTELY MAXIMALLY ENTANGLED STATES

In this section, we briefly review absolutely maximally entangled (AME) states. Let $|\Psi\rangle$ be a pure state of an N -partite quantum system described by the total Hilbert space $\mathcal{H}_{[N]} = \mathcal{H}_1 \otimes \mathcal{H}_2 \otimes \dots \otimes \mathcal{H}_N$, where $[N] = \{1, 2, \dots, N\}$. Each subsystem \mathcal{H}_i is assumed to have the same dimension d . In the computational basis $\{|j_1, j_2, \dots, j_N\rangle : j_i \in \{0, 1, \dots, d-1\}\}$, the state $|\Psi\rangle$

can be expressed as

$$|\Psi\rangle = \sum_{j_1, j_2, \dots, j_N=0}^{d-1} c_{j_1, j_2, \dots, j_N} |j_1, j_2, \dots, j_N\rangle, \quad (1)$$

where $c_{j_1, j_2, \dots, j_N} \in \mathbb{C}$ are the complex amplitudes satisfying the normalization condition

$$\sum_{j_1, j_2, \dots, j_N=0}^{d-1} |c_{j_1, j_2, \dots, j_N}|^2 = 1.$$

The reduced density matrix ρ_S of a subsystem S consisting of k parties is obtained by tracing out the remaining parties:

$$\rho_S = \text{Tr}_{S^c} (|\Psi\rangle\langle\Psi|), \quad (2)$$

where S^c denotes the complement of S in $[N]$. For the subsystem composed of the first k parties, the reduced density matrix can be expressed as

$$\rho_{[k]} = \frac{1}{d^k} AA^\dagger, \quad (3)$$

where $[k] = \{1, 2, \dots, k\}$, and A is a $d^k \times d^{N-k}$ matrix defined by its elements $(A)_{j_{k+1}, \dots, j_N}^{j_1, j_2, \dots, j_k}$

$$= \langle j_1, j_2, \dots, j_k | A | j_{k+1}, \dots, j_N \rangle = \sqrt{d^k} c_{j_1, j_2, \dots, j_N}. \quad (4)$$

The reduced density matrix ρ_S for any other subsystem S of k parties can be obtained by reshaping the matrix A . Let the subsystem S be written as $S = \{\sigma(1), \sigma(2), \dots, \sigma(k)\}$, where σ is a permutation of the N subsystem indices. The permutation corresponding to a given subset S is not unique; however, since the remaining parties are traced out, their ordering under σ is irrelevant.

The action of the permutation σ on the N -partite state yields

$$P_\sigma |\Psi\rangle = \frac{1}{\sqrt{d^k}} \sum_{j_1, j_2, \dots, j_N=0}^{d-1} (A^{R_\sigma})_{j_{\sigma(k+1)}, \dots, j_{\sigma(N)}}^{j_{\sigma(1)}, j_{\sigma(2)}, \dots, j_{\sigma(k)}} \times |j_{\sigma(1)}, j_{\sigma(2)}, \dots, j_{\sigma(N)}\rangle, \quad (5)$$

where P_σ is the permutation operator acting as $P_\sigma |j_1, j_2, \dots, j_N\rangle = |j_{\sigma(1)}, j_{\sigma(2)}, \dots, j_{\sigma(N)}\rangle$. After applying this permutation, the subsystem S occupies the first k positions, and its reduced density matrix is given by

$$\rho_S = \frac{1}{d^k} A^{R_\sigma} (A^{R_\sigma})^\dagger, \quad (6)$$

where

$$(A^{R_\sigma})_{j_{\sigma(k+1)}, \dots, j_{\sigma(N)}}^{j_{\sigma(1)}, j_{\sigma(2)}, \dots, j_{\sigma(k)}} = (A)_{j_{k+1}, \dots, j_N}^{j_1, j_2, \dots, j_k}. \quad (7)$$

These reshaping operations can be viewed as generalizations of the realignment and partial transpose operations [41, 42].

The subsystem linear entropy, defined as

$$E_L(\rho_S) = 1 - \text{Tr}(\rho_S^2),$$

quantifies the entanglement between a subsystem S and its complement S^c . It ranges from 0 for product states to $1 - 1/d^{|S|}$ for maximally entangled states, where $|S|$ denotes the cardinality of S . If the subsystem S is maximally entangled with its complement S^c , the reduced density matrix ρ_S is proportional to identity operator, that is, $\rho_S \propto \mathbb{I}_{d^{|S|}}$, assuming $|S| \leq |S^c|$. Requiring maximal entanglement for all such bipartitions defines a class of highly entangled states known as k -uniform states, and, in the special case where $k = \lfloor N/2 \rfloor$, as absolutely maximally entangled states.

Definition 1. An N -party state $|\Psi\rangle \in \mathcal{H}_{[N]}$ is k -uniform if the reduced density matrix $\rho_S = \frac{1}{d^{|S|}} \mathbb{I}_{d^{|S|}}$ for any subset $S \subset [N]$ with $|S| \leq k \leq \lfloor N/2 \rfloor$. If $k = \lfloor N/2 \rfloor$, the state is an absolutely maximally entangled state, denoted by AME(N, d).

If $|\Psi\rangle$ is a k -uniform state, then for every subsystem S with $|S| = k \leq \lfloor N/2 \rfloor$, the reduced density matrix satisfies $\rho_S = \frac{1}{d^{|S|}} \mathbb{I}_{d^{|S|}} = \frac{1}{d^{|S|}} A^{R_\sigma} (A^{R_\sigma})^\dagger$, for all permutations $\sigma \in \mathcal{S}_N$. Hence, each reshaped matrix A^{R_σ} is an isometry. Conversely, if all reshaped matrices A^{R_σ} are isometries for every $\sigma \in \mathcal{S}_N$, then the state $|\Psi\rangle$ is k -uniform. For even N and $k = N/2$, corresponding to absolutely maximally entangled (AME) states, the matrix A is referred to as a *multiunitary matrix* [25]. In practice, it is unnecessary to consider all possible $N!$ permutations. If A^{R_σ} is an isometry, then so is $A^{R_{\sigma'}}$ for any σ' related to σ by independent rearrangements of the first k and last $N - k$ indices, i.e., $\sigma' = (\sigma_1 \times \sigma_2) \circ \sigma$, where $\sigma_1 \in \mathcal{S}_k$, $\sigma_2 \in \mathcal{S}_{N-k}$. Therefore, it suffices to consider permutations from the quotient set $\mathcal{S}_N / (\mathcal{S}_k \times \mathcal{S}_{N-k})$. The size of this quotient set is $\binom{N}{k}$, so only $\binom{N}{k}$ distinct permutations — or equivalently, distinct bipartitions — need to be considered.

Since A^{R_σ} is an isometry, its rank is d^k . This implies that the minimum number of nonzero coefficients of the state $|\Psi\rangle$ in the computational basis—that is, its support—is at least d^k . k -uniform states that achieve this bound are called *minimal support k -uniform states*. In the case of AME states, the subclass of minimal support AME states is of particular interest due to their connection with maximum distance separable (MDS) codes [4].

Classical combinatorial designs such as Latin squares, orthogonal Latin squares and orthogonal arrays [25–27] are used to construct AME states. A Latin square (LS) of order d is a $d \times d$ array filled with d distinct symbols, each occurring exactly once in every row and column. Two Latin squares of the same order are said to be orthogonal if, when superimposed, every ordered pair of symbols occurs exactly once. Orthogonal arrays (OA) are generalization of orthogonal Latin squares (OLS). An orthogonal array denoted by OA(r, N, d, k) is an $r \times N$ array of d distinct symbols such that in every $r \times k$ array each

k -tuple of d symbols appears exactly the same number of times. A Latin square of order d is an $\text{OA}(d^2, 3, d, 1)$ and a pair of Latin squares of order d is an $\text{OA}(d^2, 4, d, 2)$. Table I illustrates examples of a Latin square, a pair of orthogonal Latin squares, and an orthogonal array. To

$$\text{LS}(3) = \begin{array}{|c|c|c|} \hline 0 & 1 & 2 \\ \hline 1 & 2 & 0 \\ \hline 2 & 0 & 1 \\ \hline \end{array} \quad \text{OLS}(3) = \begin{array}{|c|c|c|} \hline (0,0) & (1,1) & (2,2) \\ \hline (1,2) & (2,0) & (0,1) \\ \hline (2,1) & (0,2) & (1,0) \\ \hline \end{array}$$

$$\text{OA}(9, 4, 3, 2) = \begin{array}{|c|c|c|c|} \hline 0 & 0 & 0 & 0 \\ \hline 0 & 1 & 1 & 1 \\ \hline 0 & 2 & 2 & 2 \\ \hline 1 & 0 & 1 & 2 \\ \hline 1 & 1 & 2 & 0 \\ \hline 1 & 2 & 0 & 1 \\ \hline 2 & 0 & 2 & 1 \\ \hline 2 & 1 & 0 & 2 \\ \hline 2 & 2 & 1 & 0 \\ \hline \end{array}$$

TABLE I: Examples of a Latin square, a pair of orthogonal Latin squares, and an orthogonal array.

give an example of the construction, the following is an AME state of four qutrits obtained from the $\text{OLS}(3)$, or equivalently from the $\text{OA}(9, 4, 3, 2)$, presented in Table I:

$$|\Psi_{4,3}\rangle = \frac{1}{3} (|0000\rangle + |0111\rangle + |0222\rangle + |1012\rangle + |1120\rangle + |1201\rangle + |2021\rangle + |2102\rangle + |2210\rangle). \quad (8)$$

The construction based on orthogonal Latin squares shows the existence of four party AME states for all $d \geq 3$, with notable exception of $d = 6$. The existence of orthogonal Latin squares of order 6, famously known as ‘‘Euler’s 36 officers problem’’, admits no classical solution [35]. A quantum solution to the problem, given by an $\text{AME}(4, 6)$ state, was first given in [33]. Subsequent work demonstrated the existence of an infinite number of LU inequivalent solutions [36], and further studies have obtained new solutions [37, 38] including an explicit analytical construction [39].

An $\text{AME}(4, 6)$ state is considered *genuinely quantum* in the sense that it cannot be constructed from a classical combinatorial designs [34]. In contrast, the $\text{AME}(4, 3)$ state given in Eq. 8 is not genuinely quantum, as it can be derived from a classical OLS. It has been shown there is only one LU equivalence class of $\text{AME}(4, 3)$ states [36]. This implies that genuine quantum $\text{AME}(4, 3)$ states do not exist.

An $\text{AME}(4, d)$ state gives rise to an $d \times d$ array of quantum states that serves as an analogue of a pair of orthogonal Latin squares, known as a quantum orthogonal Latin square (QOLS). The QOLS associated with the $\text{AME}(4, 3)$ state Eq. 8 consists of separable states. On the other hand, any QOLS of order 6 corresponding to an $\text{AME}(4, 6)$ state necessarily involves entangled

states. This generalization of classical designs has led to the development of quantum combinatorial designs including quantum Latin squares [43], quantum orthogonal Latin squares, and quantum orthogonal arrays [26]. These quantum designs may offer solution to combinatorial problems for which classical solutions do not exist. In this context, a key problem is to determine whether a given AME state, up to LU equivalence, can be derived from a classical combinatorial design or is genuinely quantum. Identifying optimal representation of an AME state within the LU equivalence class is helpful for addressing this question.

III. MINIMAL DECOMPOSITION ENTROPY OF AME STATES

In this section, we begin by briefly reviewing the minimal decomposition entropy introduced in [2]. Next, we discuss some special cases of this entropy. For AME states, a lower bound for the decomposition entropy is established. Finally, we propose a numerical algorithm for computing the minimal decomposition entropy of multipartite states.

Consider a general multipartite state $|\Psi\rangle \in \mathcal{H}_{[N]}$ of an N -party system as given in Eq. 1. The set $\{p_{j_1, j_2, \dots, j_N} = |c_{j_1, j_2, \dots, j_N}|^2\}$ constructed using the coefficients forms a probability distribution. The decomposition entropy is defined as the Rényi entropy associated with this probability distribution [2]:

$$S_q(|\Psi\rangle) = \frac{1}{1-q} \log \left(\sum_{j_1, j_2, \dots, j_N=0}^{d-1} p_{j_1, j_2, \dots, j_N}^q \right), \quad q \geq 0. \quad (9)$$

This entropy has been referred to as the Rényi-Ingarden-Urbanik entropy in [2]. The minimal decomposition entropy of a state $|\Psi\rangle$ is defined by minimizing $S_q(|\Psi\rangle)$ over all local unitary operators:

$$S_q^{\min}(|\Psi\rangle) = \min_{u_1, u_2, \dots, u_N \in \mathbb{U}(d)} S_q((u_1 \otimes u_2 \otimes \dots \otimes u_N) |\Psi\rangle), \quad (10)$$

where $u_1, u_2, \dots, u_N \in \mathbb{U}(d)$ are local unitary matrices. By definition, the minimal decomposition entropy is an LU invariant, as it remains constant for all states within an LU equivalence class.

Some special cases of the minimal decomposition entropy are discussed below:

1. $q = 0$: This case corresponds to minimal Hartley entropy, which represents the minimum support that a state can achieve within its LU equivalence class. It has been shown that for any N -party state, $Nd(d-1)/2$ coefficients can always be set to zero through suitable local unitary transformations [44]. Since S_q is a non-increasing function of q , this provides an upper bound on the minimal

decomposition entropy: $S_q^{\min} \leq \log R_{\max}$, where $R_{\max} = d^N - Nd(d-1)/2$.

2. $q = 1$: In the limit $q \rightarrow 1$, the minimal Shannon entropy is obtained. This represents the minimum entropy of outcomes over all choices of local projective measurements [45].
3. $q = \infty$: In the limit $q \rightarrow \infty$, the minimal decomposition entropy can be expressed as

$$S_\infty^{\min}(|\Psi\rangle) = -\log(\lambda), \quad (11)$$

where

$$\lambda = \max_{|\phi_{\text{sep}}\rangle} |\langle \Psi | \phi_{\text{sep}} \rangle|^2$$

is obtained by optimizing over all fully separable states $|\phi_{\text{sep}}\rangle = |\phi_1\rangle \otimes |\phi_2\rangle \otimes \dots \otimes |\phi_N\rangle$. The quantity $E_G(|\Psi\rangle) = 1 - \lambda$ defines the geometric measure of entanglement (GME) [46], which is one measure of multipartite entanglement. This establishes the relation between S_∞^{\min} and the GME:

$$E_G(|\Psi\rangle) = 1 - e^{-S_\infty^{\min}(|\Psi\rangle)}. \quad (12)$$

For $q > 1$, the minimal decomposition entropy is directly related to the inverse participation ratio (IPR), a commonly used measure of localization, defined as

$$\text{IPR}_q(|\Psi\rangle) = \sum_{j_1, j_2, \dots, j_N=0}^{d-1} p_{j_1, j_2, \dots, j_N}^q. \quad (13)$$

The functional relation between the decomposition entropy and the IPR is given by

$$S_q(|\Psi\rangle) = \frac{1}{1-q} \log(\text{IPR}_q(|\Psi\rangle)). \quad (14)$$

The IPR and decomposition entropy have been widely employed in diverse contexts, including as measures of localization in many-body systems [47–51], to probe multifractality and extract fractal dimensions [52–56], to characterize quantum phases [57–66], to detect ergodicity breaking and many-body localization [67], to study measurement-induced phase transitions and circuit dynamics [68, 69].

Proposition 1. *The minimal decomposition entropy of an AME(N, d) state is bounded below by $\lfloor N/2 \rfloor \log(d)$ for all values of q . For $q < \infty$, the lower bound is achieved if and only if the AME state is of minimal support.*

Proof. We will prove this proposition by establishing a lower bound for the decomposition entropy for various values of q . For $q = 0$, the minimal Hartley entropy $S_0^{\min} \geq \lfloor N/2 \rfloor \log(d)$. This follows from the fact that the support of any AME(N, d) state is greater than or equal to $d^{\lfloor N/2 \rfloor}$. The remaining cases are considered now.

Let $|\Psi\rangle$ be an AME(N, d) state with a decomposition as given in Eq. 1, and A be the a $d^k \times d^{(N-k)}$ matrix associated with it, where $k \leq \lfloor N/2 \rfloor$. For simplicity, we introduce multi-index notation: $\mu = \{i_1, i_2, \dots, i_k\}$ and $\nu = \{i_{k+1}, \dots, i_N\}$. In terms of the matrix elements A_ν^μ , the decomposition entropy is given by:

$$S_q(|\Psi\rangle) = \frac{1}{1-q} \log \left(\frac{1}{d^{kq}} \sum_{\mu, \nu} |A_\nu^\mu|^{2q} \right). \quad (15)$$

Since the matrix A is an isometry, we have $\sum_\nu |A_\nu^\mu|^2 = 1$ for each fixed μ . Therefore, the set $\{|A_\nu^\mu|^2\}$ for a fixed μ forms a probability distribution. We consider different values of k and bipartitions to achieve a tighter bound; the decomposition entropy does not depend on these choices.

For $q = \infty$, the decomposition entropy $S_\infty(|\Psi\rangle) = -\log(\max(|A_\nu^\mu|^2)) + k \log(d)$. Since $\sum_\nu |A_\nu^\mu|^2 = 1$ for any μ , $|A_\nu^\mu|^2 \leq 1$. This implies, $\max(|A_\nu^\mu|^2) \leq 1$. Therefore $S_\infty \geq k \log(d)$. A tighter bound is obtained when $k = \lfloor N/2 \rfloor$. Therefore, $S_\infty \geq \lfloor N/2 \rfloor \log(d)$.

The case $q = 1$ corresponds to Shannon entropy:

$$S_1(|\Psi\rangle) = - \sum_\mu \left(\sum_\nu \frac{1}{d^k} |A_\nu^\mu|^2 \log \left(\frac{1}{d^k} |A_\nu^\mu|^2 \right) \right). \quad (16)$$

Simplifying the above expression, we get

$$\begin{aligned} S_1(|\Psi\rangle) &= - \frac{1}{d^k} \sum_\mu \left(\sum_\nu |A_\nu^\mu|^2 \log(|A_\nu^\mu|^2) \right) + k \log(d) \\ &= \frac{1}{d^k} \sum_\mu S_1(\mathbf{A}_\mu) + k \log(d), \end{aligned} \quad (17)$$

where $S_1(\mathbf{A}_\mu)$ denotes the Shannon entropy of the probability distribution corresponding to the μ -th row of the matrix A . The minimum value of the first term is zero if the Shannon entropy corresponding to each row of the matrix vanishes. This can occur only when each row of matrix A contains exactly one non-zero entry of magnitude 1. This possibility happens if $k = \lfloor N/2 \rfloor$ and the corresponding AME state has minimal support. Consequently, the lower bound of S_1 is $\lfloor N/2 \rfloor \log(d)$, which is attained when the AME state has minimal support. These arguments hold for any subsystem of $\lfloor N/2 \rfloor$ parties or equivalently for any reshaping of the matrix A .

For values $0 < q < \infty$, excluding the value $q = 1$, we can write the decomposition entropy as

$$\begin{aligned} S_q(|\Psi\rangle) &= \frac{1}{1-q} \log \left(\frac{d^k}{d^{kq}} \times \frac{1}{d^k} \left(\sum_{\mu, \nu} |A_\nu^\mu|^{2q} \right) \right) \\ &= \frac{1}{1-q} \log \left(\frac{1}{d^{kq}} \sum_\mu \sum_\nu |A_\nu^\mu|^{2q} \right) + k \log(d) \end{aligned} \quad (18)$$

Let $x_\mu = \sum_\nu |A_\nu^\mu|^{2q}$. Since $\sum_\nu |A_\nu^\mu|^2 = 1$, x_μ will not vanish for any values of $q < \infty$. Therefore, we can use the logarithmic form of the arithmetic-geometric mean inequality:

$$\log \left(\frac{\sum_\mu x_\mu}{d^k} \right) \geq \frac{1}{d^k} \sum_\mu \log(x_\mu). \quad (19)$$

This leads to:

$$S_q(|\Psi\rangle) \geq \frac{1}{d^k} S_q(\mathbf{A}_\mu) + k \log(d), \quad (20)$$

where $S_q(\mathbf{A}_\mu)$ is the Rényi entropy of the probability distribution corresponding to the μ -th row of the matrix A . By similar arguments as in the $q = 1$ case, we obtain $S_q \geq \lfloor N/2 \rfloor \log(d)$, where the lower bound attained only for minimal support AME states. Combining all the results, for AME(N, d) states, we have

$$S_q^{\min} \geq \lfloor N/2 \rfloor \log(d), \quad \text{for all } q. \quad (21)$$

□

For $q = \infty$, the lower bound can be attained if at least one row of A contains a non-zero entry of magnitude 1, without imposing any constraints on the other rows. Consequently, the lower bound can be achieved even with a non-minimal support AME state. For example, the AME(4, 4) state $|O_{16}\rangle$, corresponding to a 2-unitary matrix O_{16} , which has been shown to have non-minimal support [70], still attains the minimal value $S_\infty^{\min} = \log(16) = 2 \log(4)$. In Fig. 6, a 2-unitary matrix that is LU equivalent to O_{16} is given, which has non-zero entry of magnitude 1 in one of the rows.

A. Algorithm to find minimal decomposition entropy for $q > 1$

In bipartite systems, the minimal decomposition entropy can be computed using the Schmidt coefficients [2]. However, for multipartite systems, no known analytical techniques are available to find the minimal decomposition entropy. Therefore, numerical methods are employed. In this section, we propose an algorithm to compute the minimal decomposition entropy for $q > 1$. The algorithm leverages local optimization and gradient ascent, offering advantages over the random walk method used in [2].

The L_p -norm of a state $|X\rangle$ is given by $\|X\|_p = (\sum_i |x_i|^p)^{1/p}$, where $x_i = \langle i|X\rangle$ are the coefficients in the basis $\{|i\rangle\}$. The L_p norm of a matrix is similarly defined: $\|A\|_p = (\sum_{i,j} |A_{i,j}|^p)^{1/p}$. Expressing the decomposition entropy in terms of the L_p -norm of $|\Psi\rangle$ for $p = 2q$ gives

$$S_q(|\Psi\rangle) = \frac{1}{1-q} \log \left((\| |\Psi\rangle \|_{2q})^{2q} \right). \quad (22)$$

Similarly, the minimal decomposition entropy

$$S_q^{\min}(|\Psi\rangle) = \min_{u_1, \dots, u_N \in \mathbb{U}(d)} \frac{1}{1-q} \log \left((\|(u_1 \otimes \dots \otimes u_N)|\Psi\rangle\|_{2q})^{2q} \right). \quad (23)$$

For $q > 1$, this problem is equivalent to the maximization problem

$$\mathcal{L}_q^{\max}(|\Psi\rangle) = \max_{u_1, \dots, u_N \in \mathbb{U}(d)} (\|(u_1 \otimes \dots \otimes u_N)|\Psi\rangle\|_{2q})^{2q}. \quad (24)$$

The core of our algorithm is to find $\mathcal{L}_q^{\max}(|\Psi\rangle)$. For a fixed set of matrices $\{u_2^{(0)}, \dots, u_N^{(0)}\}$, the above maximization problem is $\mathcal{L}_q^{\max}(|\Psi\rangle) \big|_{u_2^{(0)}, \dots, u_N^{(0)}}$

$$= \max_{u_1 \in \mathbb{U}(d)} \left(\|(u_1 \otimes u_2^{(0)} \otimes \dots \otimes u_N^{(0)})|\Psi\rangle\|_{2q} \right)^{2q}. \quad (25)$$

We observe that

$$\left(\|(u_1 \otimes u_2^{(0)} \otimes \dots \otimes u_N^{(0)})|\Psi\rangle\|_{2q} \right)^{2q} = (\|u_1 M_1\|_{2q})^{2q},$$

where the matrix M_1 of order $d \times d^{N-1}$ defined by its elements

$$\langle l_1 | M_1 | l_2, \dots, l_N \rangle = \langle l_1, l_2, \dots, l_N | (\mathbb{I}_d \otimes u_2^{(0)} \otimes \dots \otimes u_N^{(0)}) |\Psi\rangle.$$

Therefore,

$$\mathcal{L}_q^{\max}(|\Psi\rangle) \big|_{u_2^{(0)}, \dots, u_N^{(0)}} = \max_{u_1 \in \mathbb{U}(d)} (\|u_1 M_1\|_{2q})^{2q}. \quad (26)$$

This maximization problem is related to the principle component analysis of complex matrices using L_p -norm, referred to as complex L_p -PCA. The L_p -PCA problem for real matrices is investigated in [71]. For our purpose, the method is extended to the case of complex matrices. A detailed complex L_p -PCA algorithm is given in the appendix.

The complex L_p -PCA problem enables us to find a unitary matrix $u_1^{(1)}$ such that the norm in Eq. 26 is maximized. That is,

$$(u_1^{(1)})^\dagger = \operatorname{argmax}_{\theta \in \mathbb{U}(d)} (\|\theta^\dagger M_1\|_{2q})^{2q}. \quad (27)$$

Following a similar approach, the matrices $u_i^{(j+1)}$ are found using the complex L_p -PCA algorithm for $i = 1, 2, \dots, N$, and each iteration step $j = 0, 1, 2, \dots$. Once the algorithm converges, the final step involves applying the obtained local unitary matrices to the original state in order to compute the decomposition entropy. The detailed algorithm is provided below:

Algorithm

Initialize random unitary matrices $u_1^{(0)}, u_2^{(0)}, \dots, u_N^{(0)} \in \mathbb{U}(d)$

For $j = 1, 2, \dots$

For $i = 1, 2, \dots, N$

$$(u_i^{(j+1)})^\dagger = \operatorname{argmax}_{\theta \in \mathbb{U}(d)} (\|\theta^\dagger M_i\|_{2q})^{2q},$$

where M_i is a $d \times d^{N-1}$ matrix with entries

$$\langle l_i | M_i | l_1, \dots, l_{i-1}, l_{i+1}, \dots, l_N \rangle = \langle l_1, \dots, l_N | Q_i | \Psi \rangle$$

where $Q_i = (u_1 \otimes \dots \otimes u_{i-1} \otimes \mathbb{I}_d \otimes u_{i+1} \otimes \dots \otimes u_N)$.

The maximization at each step ensures that the algorithm converges. However, this does not guarantee reaching the global maximum, as a local maximization is performed in each step. Multiple runs of the algorithm with randomly chosen seed unitary matrices may be necessary to find the global maximum.

IV. NUMERICAL RESULTS

In this section, we present numerical results, primarily focusing on the cases $q = 2$ and $q = \infty$. The distribution of $S_2, S_2^{\min}, S_\infty$, and S_∞^{\min} for both typical states and AME states are computed for various values of N and d . We also discuss examples of optimal representations of AME states, highlighting their usefulness in obtaining sparse representations and in determining whether a given AME state is genuinely quantum.

A. Minimal decomposition entropy for $q = 2$

The probability distributions of the estimations of S_2 and S_2^{\min} for Haar-random states and random AME states are obtained by constructing ensembles of such states. The ensemble of AME states is produced by applying the algorithm described in Appendix A. The minimal decomposition entropy, S_2^{\min} , is calculated using the algorithm proposed in this work. Results for qubit, qutrit, and ququad systems are presented in Figs. 1, and the corresponding ensemble averages of are listed in Table II.

Some special cases are noted first. It is known that all AME(3, 2) states are LU equivalent to the GHZ state [1], which is given by

$$|GHZ\rangle = \frac{1}{\sqrt{2}} (|000\rangle + |111\rangle).$$

Since the GHZ state has minimal support, the minimal decomposition entropy S_q^{\min} for any AME(3, 2) state is $\log(2)$ for all q . As a result, the distribution of S_2^{\min} of AME(3, 2) states is a delta function at $\log(2)$. Similarly, all AME(4, 3) states are LU equivalent to the minimal

support state given in Eq. 8 [36], and thus the minimal decomposition entropy for any AME(4, 3) state is $S_q^{\min} = \log(9)$. To demonstrate this, the convergence of the algorithm for twenty random AME(4, 3) states is plotted in Fig. 3. The algorithm provides a set of four local unitary matrices that connect a given random AME(4, 3) state to a minimal support state. For four qubits, no AME states exists [18], and the data for Haar random states is presented in Fig. 1b, which shows the distribution of S_2^{\min} for typical states.

We next examine the distribution of the minimal decomposition entropy S_2^{\min} . In the ensemble of Haar random three qubit states, approximately 45% of states are found to have $S_2^{\min} \geq \log(2)$. For three qutrit states, the distribution of S_2^{\min} of Haar random states and AME(3, 3) states shows significant overlap. However, in the case of four qutrits and four ququad system, majority of Haar random states in the ensemble exhibit larger S_2^{\min} values compared to AME states. This observation suggests that, in these cases, Haar-random states are more entangled than AME states, while AME states can be transformed into a more optimal form compared to typical Haar-random states.

For AME(4, 4) states, the distribution of S_2^{\min} is highly irregular. This irregularity may reflect the underlying structure of the set of LU-equivalence classes, or it may be an artifact of the state generation algorithm. Further investigation, potentially involving analytical methods, is required to resolve this behavior.

Extremal states that maximize S_2^{\min} are of particular interest when investigating maximally entangled states with respect to this measure. This topic has been explored in previous works [2, 40]. In Table III, we present data on the maximum values of S_2^{\min} observed in both the ensemble of Haar-random states and AME states. We have identified states that exhibit higher S_2^{\min} values than those previously known. These states are detailed in [73], and the corresponding values are provided in Table III.

B. Minimal decomposition entropy for $q = \infty$

To calculate the minimal decomposition entropy S_∞^{\min} of a given state $|\Psi\rangle$, we employ the seesaw algorithm [74] and use the relation in Eq. 11. The seesaw algorithm, originally proposed to find the GME, is used to identify the nearest fully separable state $|\phi_{\text{sep}}\rangle$ to a the N -partite state $|\Psi\rangle$. The overlap $|\langle \Psi | \phi_{\text{sep}} \rangle|^2$ is then used to determine S_∞^{\min} . The relationship between the minimal decomposition entropy S_∞^{\min} and the GME is provided in Eq. 12, highlighting that studying S_∞^{\min} is equivalent to investigating the GME. The GME has been studied extensively, and a recent review of this can be found in [75].

The distributions of S_∞ and S_∞^{\min} for qubit, qutrit, and ququad systems are shown in Fig. 2, with the corresponding ensemble averages listed in Table II. It is observed

	$\langle S_2 \rangle_H$	$\langle S_2^{\min} \rangle_H$	$\langle S_2 \rangle_{\text{AME}}$	$\langle S_2^{\min} \rangle_{\text{AME}}$	$\langle S_\infty \rangle_H$	$\langle S_\infty^{\min} \rangle_H$	$\langle S_\infty \rangle_{\text{AME}}$	$\langle S_\infty^{\min} \rangle_{\text{AME}}$
Three qubits	1.531	0.648	1.710	0.693	1.113	0.379	1.381	0.693
Four qubits	2.160	1.200	–	–	1.589	0.694	–	–
Three qutrits	2.651	1.384	2.782	1.480	1.965	0.852	2.169	1.304
Four qutrits	3.719	2.531	3.875	2.197	2.812	1.506	3.123	2.197
Four ququads	4.857	3.639	4.963	3.341	3.751	2.176	3.995	2.896

TABLE II: The average values of decomposition entropy S_2 and its minimal value S_2^{\min} of Haar random states and random AME states (denoted by subscripts H and AME, respectively) for various cases. For four qubits, AME states do not exist, and the absence of values is denoted by –.

	Ensemble $\max(S_2^{\min})_H$	Ensemble $\max(S_2^{\min})_{\text{AME}}$	Known $\max(S_2^{\min})$ [2, 40]	Ensemble $\max(S_\infty^{\min})_H$	Ensemble $\max(S_\infty^{\min})_{\text{AME}}$	Known $\max(S_\infty^{\min})$ [40, 72]
Three qubits	1.257*	0.693	1.108	0.768	0.693	$\log(9/4) \approx 0.810$
Four qubits	1.747	–	$\log(6) \approx 1.791$	1.175	–	$\log(9/2) \approx 1.504$
Three qutrits	1.789	1.944*	$\log(6) \approx 1.791$	1.275	1.529	$\log(6) \approx 1.791$
Four qutrits	2.893*	2.197	$\log(12) \approx 2.484$	1.843	2.197	$\log(9) \approx 2.197$
Four ququads	3.904*	3.518	†	2.431	2.985	$\log(24) \approx 3.178$

TABLE III: The maximum values of minimal decomposition entropy S_2^{\min} and S_∞^{\min} for Haar random states and random AME states (denoted by subscripts H and AME, respectively), computed over different ensembles. Previously conjectured or numerically found maximum values are provided for comparison. For four qubits, AME states do not exist, and the absence of values is denoted by –. Entries marked with * indicate newly obtained maximum values, and those marked with † indicate values that are not known.

that, for the cases considered, typical AME states exhibit higher S_∞^{\min} compared to Haar random states. In other words, in terms of both GME and minimal decomposition entropy, AME states are more entangled than Haar random states.

The maximal values of the GME and minimal decomposition entropy S_∞^{\min} have been previously investigated [2, 40, 72]. In Table III, we present the maximum values obtained from the ensembles of Haar random states and AME states considered in our study. We did not find any new states with S_∞^{\min} exceeding the previously known maximum values. However, a new four-ququad AME state has been identified with $S_\infty^{\min} = 2.985$, which is higher than the previously reported value of $S_\infty^{\min} = \log(16) \approx 2.772$ [72]. The state is provided in [73].

C. Minimal decomposition entropy for finite $q > 1$

The algorithm proposed in this work can be used to compute S_q^{\min} for other values of $q > 1$. To demonstrate this, we plot S_q and S_q^{\min} for a three qutrit Haar random state and an AME(3,3) state in Fig. 4, with $1.5 \leq q \leq 100$ in increments of 0.5. The value of the minimal decomposition entropy at $q = \infty$ is computed independently using the seesaw algorithm. As q becomes larger, it is observed that the minimal decomposition entropy converges to the value obtained through the seesaw algorithm in each case.

D. Optimal representation of AME states

The state with minimum decomposition entropy, S_2^{\min} , provides an optimal representation in the sense that the entropy is minimized in the corresponding product basis, often yielding a simpler and sparser description of the state. The algorithm presented in this work identifies a product basis that achieves this minimum. It is important to note that this optimal form is not unique: multiplying the state by local diagonal unitaries or applying local permutation matrices, for example, does not change the decomposition entropy. In principle, the Hartley entropy is the most direct measure of sparsity, as it simply counts the number of nonzero coefficients; minimizing it therefore yields the representation with truly minimal support within a given LU-equivalence class. However, the Hartley entropy is difficult to optimize in practice, and for this reason one typically minimizes the Shannon entropy or decomposition entropies for other values of q .

We provide several examples illustrating how the algorithm for computing S_2^{\min} yields a simpler and sparser representation of an AME state, often with significantly reduced support compared to the original form. The first example, shown in Fig. 5, displays a 2-unitary matrix corresponding to a random AME(4,3) state alongside the final matrix obtained after applying the algorithm. In this case, the original state has support 81, whereas the transformed state attains minimal support, as expected.

As another example, we consider the AME(4,4) state $|O_{16}\rangle$, corresponding to the 2-unitary matrix O_{16} given in

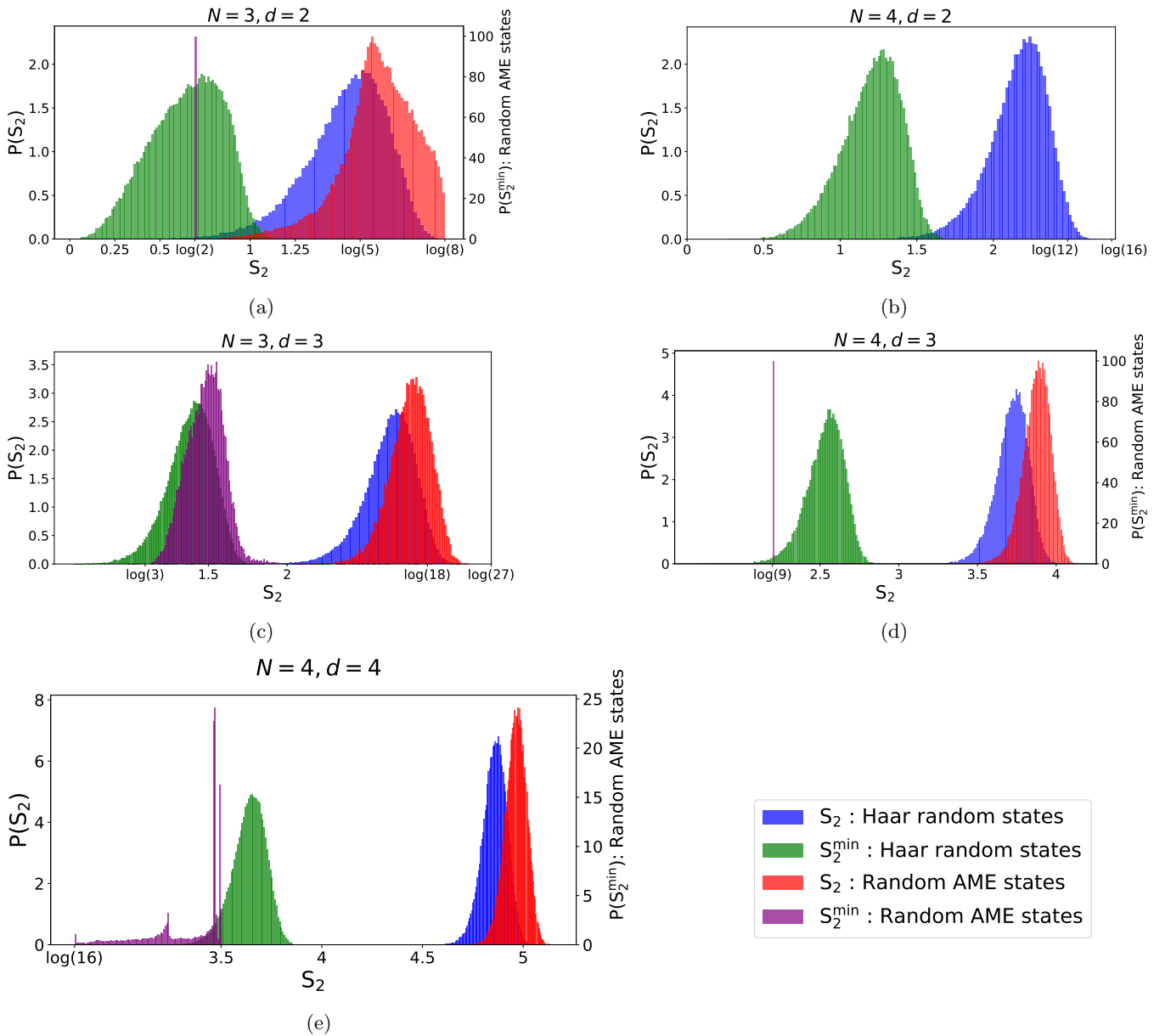


FIG. 1: Distribution of S_2 and S_2^{\min} for Haar random states and random AME states in (a) three qubits, (b) four qubits, (c) three qutrits, (d) four qutrits, and (e) four ququads. For the ensembles of AME states, the lower bound of S_2 for $\text{AME}(N, d)$ states, given by $\log(d^{\lfloor N/2 \rfloor})$, is indicated. The upper bound for S_2 , $\log(d^N)$, and the known upper bound for S_2^{\min} , $\log(d^N - \frac{1}{2}Nd(d-1))$, are included wherever possible. The ensembles of $\text{AME}(3, 3)$, $\text{AME}(4, 3)$, and $\text{AME}(4, 4)$ consist of 2.5×10^4 states, while all other Haar random and AME state ensembles contain 10^5 states.

[70]. Depictions of the original state $|O_{16}\rangle$ and the state obtained after applying our algorithm are shown in Fig. 6. In this case, the final state has support 28, compared to 64 for the original. The algorithm-derived state can be further simplified by removing complex phases via local diagonal unitaries and by applying local permutations, yielding an even simpler representation. All of these versions—the original, the algorithm output, and the fully refined state—are provided in Appendix C. Additional examples, including the cases of $\text{AME}(4, 6)$, $\text{AME}(5, 2)$,

and $\text{AME}(6, 2)$, are presented in the appendix D. The quantum states and the local unitary matrices found using the algorithm are provided in [73].

Obtaining a simpler representation of an AME state is useful for determining whether the state is genuinely quantum or whether it can be constructed from a classical combinatorial structure. It is known that minimal-support AME states can be constructed from orthogonal arrays [76]. Since the minimal decomposition entropy S_2^{\min} attains its lower bound only for minimal-support

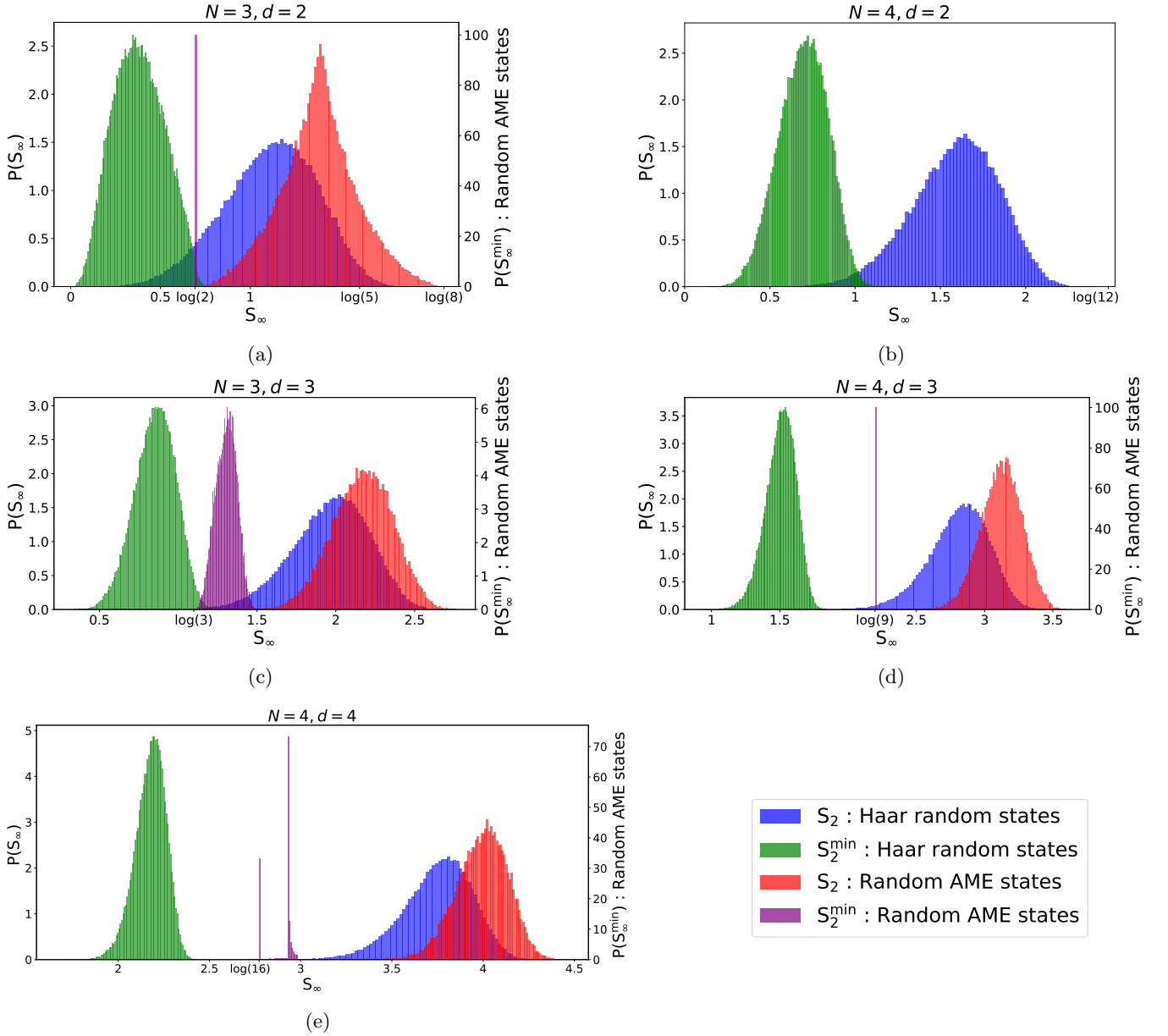


FIG. 2: Distribution of S_∞ and S_∞^{\min} for Haar random states and random AME states in (a) three qubits, (b) four qubits, (c) three qutrits, (d) four qutrits, and (e) four ququads. For the ensembles of AME states, the lower bound of S_2 for $\text{AME}(N, d)$ states, given by $\log(d^{\lfloor N/2 \rfloor})$, is indicated. The upper bound for S_2 , $\log(d^N)$, and the known upper bound for S_2^{\min} , $\log(d^N - \frac{1}{2}Nd(d-1))$, are included wherever possible. The ensembles of $\text{AME}(3, 3)$, $\text{AME}(4, 3)$, and $\text{AME}(4, 4)$ consist of 2.5×10^4 states, while all other Haar random and AME state ensembles contain 10^5 states.

states, any state that achieves this minimum is therefore not genuinely quantum. In the cases we examined, this implies that there are no genuinely quantum AME states for three qubits or for four qutrits. In contrast, for the $\text{AME}(3, 3)$ and $\text{AME}(4, 4)$ families, we find that most states in the ensemble are genuinely quantum.

V. CONCLUSIONS

The decomposition entropy S_q^{\min} provides a measure of how localized a quantum state is within a given basis. When minimized over all local unitaries, it serves as an entanglement measure and yields an optimal representative of the state within its LU-equivalence class, making it a useful tool for exploring LU equivalence. For $q = \infty$, the minimal decomposition entropy is directly related to the geometric measure of entanglement. In this work,

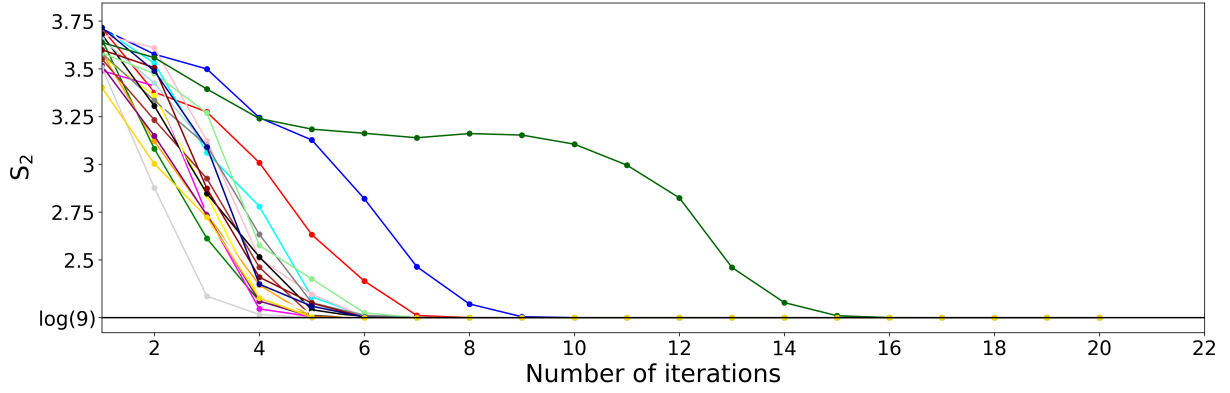


FIG. 3: The convergence of the algorithm for twenty random AME(4,3) states is shown, with each state represented by a different color. The decomposition entropy at each iteration step is plotted. The plot demonstrates convergence of S_2 to the theoretical value $\log(9)$.

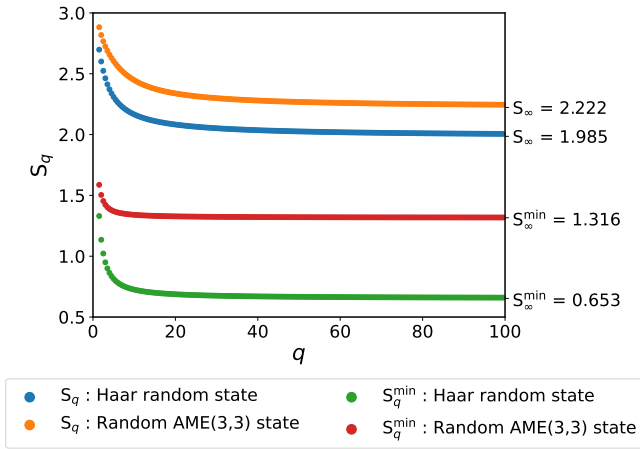


FIG. 4: The minimal decomposition entropy S_q and S_q^{\min} as a function of q for a Haar random three qutrit state and a random AME(3,3) state plotted for $q > 1$ with a step size 0.5. The values at $q = \infty$ are marked on the right side.

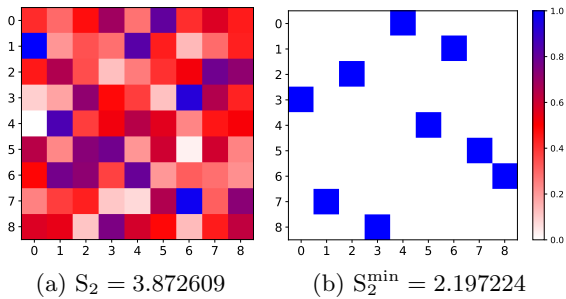


FIG. 5: (a) 2-unitary matrix corresponding to a random AME(4,3) state. (b) 2-unitary matrix corresponding the state obtained by applying the algorithm. Only the absolute values are shown in both cases. The values of entropy are given, and the S_2^{\min} value matches the lower bound $\log(9)$ up to five decimal places for AME(4,3) states.

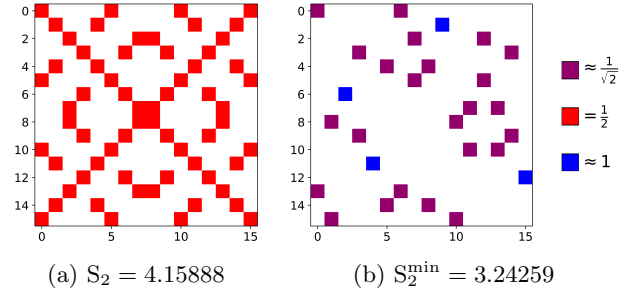


FIG. 6: (a) 2-unitary matrix O_{16} . (b) 2-unitary matrix corresponding the state obtained by applying the algorithm. Only the absolute values are shown in each cases. The values of entropy are given. The support of the final state is 28 compared to 64 of the original state.

we examined the minimal decomposition entropy for a family of highly entangled multipartite states known as absolutely maximally entangled (AME) states.

An algorithm was introduced to determine the minimal decomposition entropy S_q^{\min} for finite $q > 1$, and the known seesaw algorithm was employed to compute S_∞^{\min} . We investigated Haar-random states and AME states of qubits, qutrits, and ququads for the cases $q = 2$ and $q = \infty$. For three qutrits and four ququads, we observed that S_2^{\min} is larger for Haar-random states than for AME states, indicating that AME states can be more localized in these scenarios. In both ensembles, typical AME states were found to have larger S_∞^{\min} , and thus larger geometric entanglement, than their Haar-random counterparts. We also identified new states exhibiting higher values of both S_2^{\min} and S_∞^{\min} . Furthermore, we demonstrated that the algorithm is effective in obtaining optimal representations of AME states and in determining whether a given AME state is genuinely quantum – that is, not realizable from a classical combinatorial design. For the AME(3,3) and AME(4,4) families, we found that most states are genuinely quantum.

The approach and algorithm developed in this work are not limited to AME states and can be applied to general multipartite quantum systems. While our analysis has focused on relatively small values of N and d , the method can be readily extended to larger systems and higher-dimensional subsystems. Obtaining optimal or sparser representations of such states can provide valuable insights into their entanglement structure and other key properties. However, because the algorithm relies on a greedy optimization strategy, it may fail to converge to the global minimum and can become trapped in local minima, particularly for systems with many parties or higher local dimensions. This limitation underscores the need for further analytical and algorithmic developments.

The theoretical upper bounds for the minimal decomposition entropy remain unknown for AME states and, more broadly, for many multipartite systems with general N and d . The problem of finding maximally entangled states with respect to the minimal decomposition entropy remains largely open.

DATA AVAILABILITY

Certain data and Python code that support the findings of this study are openly accessible on GitHub under the GNU General Public License v3.0 [73]. Due to the large size of the remaining datasets, they are not publicly available. However, the code and algorithms required to generate and verify these datasets are provided in the repository.

ACKNOWLEDGEMENT

N.R. acknowledges funding received from the Center for Quantum Information, Communication, and Computing, IIT Madras, during his time at the institute, and thanks Arul Lakshminarayan for valuable discussions and insightful comments on the manuscript.

Appendix A: Algorithm to generate k -uniform and AME states

To construct k -uniform and absolutely maximally entangled (AME) states, we develop an algorithm inspired by the methods introduced in [77] for generating dual-unitary and 2-unitary matrices. Consider a complex matrix $A \in M_{m,n}(\mathbb{C})$ with $m \leq n$ and normalization condition $\text{Tr}(A^\dagger A) = m$. Let $A = UDV$ be the singular value decomposition of A , where $D_{ij} = s_i \delta_{ij}$ for $i = 1, \dots, m$ and $j = 1, \dots, n$, with s_i representing the singular values of A . The matrices U and V are unitary, with dimensions $m \times m$ and $n \times n$, respectively. We define the map

$$\text{Iso}(A) = U[I_m|0]V. \quad (\text{A1})$$

where $[I_m|0]$ represents the $m \times n$ matrix obtained by concatenating the identity matrix I_m with an $m \times (n-m)$ zero block. The matrix $\text{Iso}(A)$ gives the isometry closest to A in the Frobenius norm, corresponding to the solution of the a rectangular variant of the orthogonal Procrustes problem [78].

The nuclear norm of a matrix is defined as the sum of its singular values,

$$\|A\|_* = \sum_{i=1}^m \sigma_i. \quad (\text{A2})$$

It can equivalently be expressed as

$$\|A\|_* = \text{Tr}(A^\dagger \text{Iso}(A)). \quad (\text{A3})$$

The nuclear norm $\|A\|_*$ attains its maximum value m when A is an isometry. To see this, note that the normalization condition $\text{Tr}(A^\dagger A) = m$ implies $\sum_{i=1}^m s_i^2 = m$. Using Cauchy-Schwarz inequality,

$$\sum_{i=1}^m s_i \leq \sqrt{m} \sqrt{\sum_{i=1}^m s_i^2} = m,$$

and equality holds if and only if $s_i = 1$ for all i , that is, when A is an isometry.

Additionally,

$$\|A\|_* = \text{Tr}(A^\dagger \text{Iso}(A)) \geq \text{Re}(\text{Tr}(A^\dagger Q)) \quad (\text{A4})$$

for any isometry $Q \in M_{m,n}(\mathbb{C})$. Indeed,

$$\begin{aligned} \text{Re}(\text{Tr}(A^\dagger Q)) &= \text{Re}(\text{Tr}(V^\dagger D U^\dagger Q)) \\ &= \text{Re}(\text{Tr}(D Q')) \quad (Q' = U^\dagger Q V^\dagger) \\ &= \text{Re}\left(\sum_{i=1}^m s_i Q'_{ii}\right). \end{aligned}$$

Since

$$\text{Re}\left(\sum_{i=1}^m s_i Q'_{ii}\right) \leq \left|\sum_{i=1}^m s_i Q'_{ii}\right| \leq \left(\sum_{i=1}^m s_i |Q'_{ii}|\right)$$

and for an isometry Q' , one has $|Q'_{ii}| \leq 1$, it follows that

$$\text{Re}(\text{Tr}(A^\dagger Q)) \leq \sum_{i=1}^m s_i = \text{Tr}(A^\dagger \text{Iso}(A)). \quad (\text{A5})$$

Consider an N -partite state $|\Psi\rangle$, and define its associated $d^k \times d^{N-k}$ matrix A as given in Eq 4, where $k \leq \lfloor N/2 \rfloor$. For AME states k is chosen as $k = \lfloor N/2 \rfloor$. We introduce the following objective function:

$$f(A) = \mathcal{N} \sum_{\sigma \in \mathcal{S}_N^k} \|A^{R_\sigma}\|_*, \quad (\text{A6})$$

where $\mathcal{N} = \frac{k!(N-k)!}{d^k N!}$ and $\mathcal{S}_N^k = \mathcal{S}_N / (\mathcal{S}_k \times \mathcal{S}_{N-k})$.

The norm $\|A^{R_\sigma}\|_*$ reaches its maximum value if and only if A^{R_σ} is an isometry. Consequently, $f(A)$ attains its maximal value of 1 when all the matrices A^{R_σ} corresponding to permutations $\sigma \in \mathcal{S}_N^k$ are isometries – equivalently, when the state associated with the matrix A is k -uniform. The normalization factor \mathcal{N} is chosen such that maximum value of $f(A)$ is 1; this choice accounts for the size of the set \mathcal{S}_N^k , which contains $N!/(k!(N-k)!)$ permutations, and the fact that the nuclear norm of a $d^k \times d^{N-k}$ isometry equals d^k .

We find an algorithm that maximize $f(A)$ and it is given now.

Algorithm to generate k -uniform states

Initialize random $d^k \times d^{(N-k)}$ isometry A_0 .

For $i = 1, 2, \dots$

$$A_i = \mathcal{N} \sum_{\sigma \in \mathcal{S}_N^k} \left(\text{Iso} \left(A_{i-1}^{R_\sigma} \right) \right)^{R_{\sigma^{-1}}}$$

Repeat until convergence of $f(A_i)$

The iterative update

$$A_{i+1} = \mathcal{N} \sum_{\sigma \in \mathcal{S}_N^k} \left(\text{Iso} \left(A_i^{R_\sigma} \right) \right)^{R_{\sigma^{-1}}}$$

ensures that $f(A_i)$ forms a non-decreasing sequence. The objective function $f(A_i)$ can be expressed as

$$\begin{aligned} f(A_i) &= \mathcal{N} \sum_{\sigma \in \mathcal{S}_N^k} \text{Tr} \left(\left(A_i^{R_\sigma} \right)^\dagger \text{Iso} \left(A_i^{R_\sigma} \right) \right) \\ &= \mathcal{N} \text{Tr} \left(A_i^\dagger \sum_{\sigma \in \mathcal{S}_N^k} \left(\text{Iso} \left(A_i^{R_\sigma} \right) \right)^{R_{\sigma^{-1}}} \right) \quad (\text{A7}) \\ &= \text{Tr} \left(A_i^\dagger A_{i+1} \right). \end{aligned}$$

The identity $\text{Tr} \left(A^{R_\sigma \dagger} B \right) = \text{Tr} \left(A^\dagger B^{R_\sigma} \right)$ is used in this derivation. Similarly,

$$\begin{aligned} f(A_{i-1}) &= \text{Tr} \left(A_{i-1}^\dagger A_i \right) = \text{Tr} \left(A_i^\dagger A_{i-1} \right) \\ &= \mathcal{N} \sum_{\sigma \in \mathcal{S}_N^k} \text{Tr} \left(\left(A_i^{R_\sigma} \right)^\dagger \text{Iso} \left(A_{i-2}^{R_\sigma} \right) \right). \end{aligned}$$

From the relation stated in Eq. A4, it follows that

$$\text{Tr} \left(\left(A_i^{R_\sigma} \right)^\dagger \text{Iso} \left(A_i^{R_\sigma} \right) \right) \geq \text{Tr} \left(\left(A_i^{R_\sigma} \right)^\dagger \text{Iso} \left(A_{i-2}^{R_\sigma} \right) \right),$$

and hence $f(A_i) \geq f(A_{i-1})$. Although this iterative scheme guarantees that the objective function is non-decreasing, convergence to the global maximum is not guaranteed, and the procedure may become trapped in local maxima. To mitigate this, several runs with randomly initialized seed isometries are typically performed.

Appendix B: Principal component analysis using L_p -norm for complex matrices

Let $X = [x_1 x_2 \dots x_N]$ be a $d \times N$ complex matrix. Define the function $F_p : \mathbb{C} \rightarrow \mathbb{R}$ such that

$$F_p(W) = \|W^\dagger X\|_p^p = \sum_{i=1}^N \sum_{j=1}^m |w_j^\dagger x_i|^p, \quad (\text{B1})$$

where W is a $d \times m$ complex matrix with $W^\dagger W = \mathbb{I}_m$. Here w_j denotes the j -th column of W and \mathbb{I}_m denotes the $m \times m$ identity matrix. The L_p norm is convex for $p > 1$. Hence, the function $F_p(W)$ is convex for $p > 1$ since it is a sum of convex functions. The maximization problem is to find a W such that $F_p(W)$ is maximum:

$$(\text{Complex LP-PCA}) \quad \max_{W \in \mathbb{C}^{d \times m}, W^\dagger W = \mathbb{I}_m} F_p(W). \quad (\text{B2})$$

For $p = 2$, the problem becomes

$$F_2(W) = \sum_{i=1}^N \sum_{j=1}^m |w_j^\dagger x_i|^2 = \text{Tr} \left(W^\dagger X X^\dagger W \right). \quad (\text{B3})$$

The global optimal solution is found by solving $X X^\dagger W = W D$, where D is a diagonal matrix containing eigenvalues of $X X^\dagger$. For other values of $p > 1$, finding a solution is difficult. An algorithm is proposed by extending the methods given in [71] for complex data.

Define the Lagrangian of the problem

$$\begin{aligned} L(W, \Lambda) &= \|W^\dagger X\|_p^p + \text{Tr}(\Lambda(W^\dagger W - \mathbb{I}_m)) \\ &= \sum_{i=1}^N \sum_{j=1}^m |w_j^\dagger x_i|^p + \sum_{k,l} \lambda_{k,l} \left(w_k^\dagger w_l - \delta_{k,l} \right), \end{aligned} \quad (\text{B4})$$

where Λ is an $m \times m$ Hermitian matrix. The necessary condition for the optimal solution can be obtained by setting the derivative of the Lagrangian to zero:

$$\frac{dL}{dW^*} = 0. \quad (\text{B5})$$

Note that $\frac{dL}{dW^*} = \left(\frac{dL}{dW} \right)^*$. Define the gradient as follows

$$\nabla_{W^*} = \frac{dF_p(W)}{dW^*} = [\nabla_{w_1^*} \quad \nabla_{w_2^*} \quad \dots \quad \nabla_{w_m^*}] \quad (\text{B6})$$

where

$$\begin{aligned} \nabla_{w_k^*} &= \frac{\partial}{\partial w_k^*} \left(\sum_{i=1}^N \sum_{j=1}^m |w_j^\dagger x_i|^p \right) \\ &= \sum_{i=1}^N \frac{p}{2} (w_k^\dagger x_i)^{p/2-1} (x_i^\dagger w_k)^{p/2} x_i. \end{aligned} \quad (\text{B7})$$

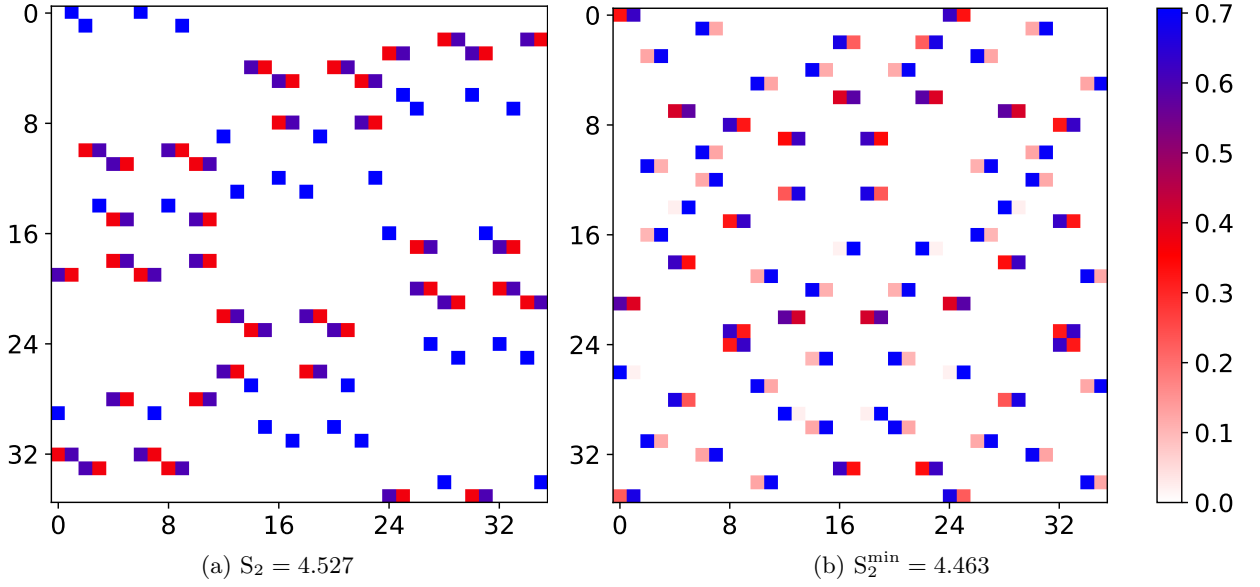


FIG. 7: (a) The 2-unitary matrix corresponding to the Golden AME state [33], presented in its simplified form. (b) The 2-unitary matrix for the state obtained after applying the algorithm. Only the absolute values are shown, and the entropy values are provided. The support of the final state is 144, compared to 112 for the original, indicating an increase in support despite the lower entropy. This is expected, as the minimum value of S_2^{\min} may not yield the state with minimal support within a given LU equivalence class.

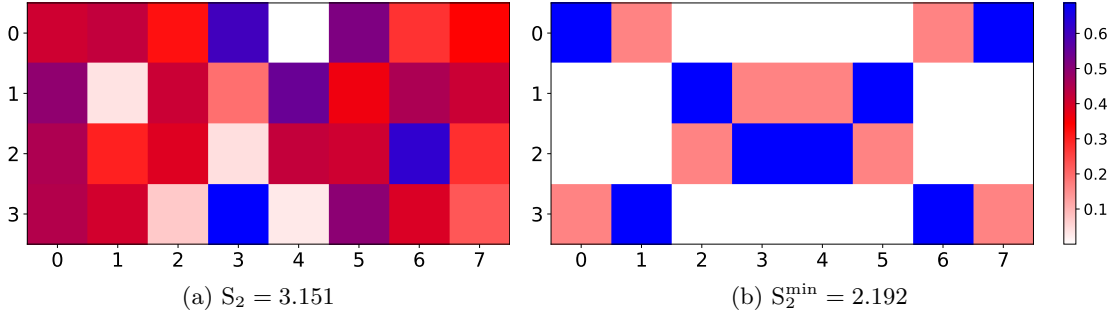


FIG. 8: (a) The isometry corresponding to a random AME(5,2) state. (b) The isometry corresponding to the same state obtained by applying the algorithm. Only the absolute values of the matrix elements are shown in each case, with entropy values provided. The support of the final state is 16, compared to 32 for the original state.

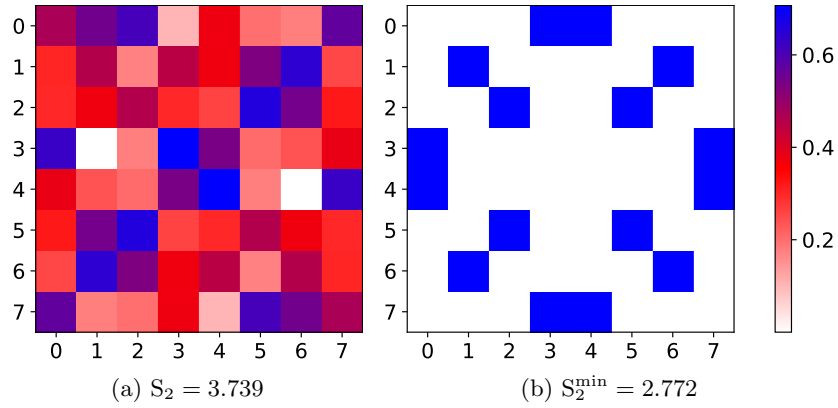


FIG. 9: (a) The 3-unitary matrix corresponding to a random AME(6,2) state. (b) The 3-unitary matrix for the same state after applying the algorithm. Only the absolute values of the matrix elements are shown, and the entropy values are given. The support of the final state is 16 compared to 64 of the original state.

Also,

$$\begin{aligned} \frac{\partial}{\partial w_q^*} \left(\sum_{k,l} \lambda_{k,l} (w_k^\dagger w_l - \delta_{k,l}) \right) &= \sum_{k,l} \lambda_{k,l} (w_l \delta_{k,q}) \\ &= \sum_l \lambda_{q,l} w_l. \end{aligned} \quad (\text{B8})$$

Therefore, the condition becomes

$$\frac{dL}{dW^*} = \nabla_{W^*} + W\Lambda = 0. \quad (\text{B9})$$

In each iteration, the matrix W is chosen by solving the optimization problem

$$W' = \underset{Q \in \mathbb{C}^{d \times m}, Q^\dagger Q = \mathbb{I}_m}{\operatorname{argmax}} \operatorname{Re} \left(\operatorname{Tr} (Q^\dagger \nabla_{W^*}) \right). \quad (\text{B10})$$

The idea is to find a W as close to ∇_{W^*} such that the the constraint $W^\dagger W = \mathbb{I}_m$ is satisfied [71]. The solution to the above optimization problem is given by

$$W' = U[I_m | \mathbf{0}] V^\dagger, \quad (\text{B11})$$

where the unitary matrices U and V are obtained from the singular value decomposition $\nabla_{W^*} = UDV^\dagger$. The iterative update ensures that $F_p(W') \geq F_p(W)$. This can be shown as follows:

The function $F_p(W)$ is convex for $p > 1$. Therefore, the first order convexity condition implies [79]

$$F_p(W') - F_p(W) \geq 2 \operatorname{Re} \left(\operatorname{Tr} ((W'^\dagger - W^\dagger) \nabla_{W^*}) \right) \quad (\text{B12})$$

Since W' is a solution of the optimization problem in Eq. B10, this gives $\operatorname{Re} \left(\operatorname{Tr} (W'^\dagger \nabla_{W^*}) \right) \geq \operatorname{Re} \left(\operatorname{Tr} (W^\dagger \nabla_{W^*}) \right)$. Therefore,

$$F_p(W') - F_p(W) \geq 0. \quad (\text{B13})$$

The algorithm is given below:

Algorithm : Complex LP-PCA

Initialize W_0 such that $W_0^\dagger W_0 = I_m$. For $i = 0, 1, \dots$

- 1) Compute $\nabla_{W_i^*}$
 - 2) SVD : $\nabla_{W_i^*} = U_i D V_i^\dagger$
 - 3) $W_{i+1} \leftarrow U_i [I_m | \mathbf{0}] V_i^\dagger$
-

The iterative update in Eq. B10 ensures that the algorithm converges.

Appendix C: AME(4, 4) states $|O_{16}\rangle$ and $|O'_{16}\rangle$

The AME(4, 4) state $|O_{16}\rangle$, corresponding to the 2-unitary matrix O_{16} , the state obtained from the algorithm $|O_{16}^{\text{alg}}\rangle$, which corresponds to the minimal entropy value, and the refined state $|O_{16}^{\text{ref}}\rangle$, obtained by removing complex phases and applying local permutations, are presented below:

$$\begin{aligned} |O_{16}\rangle = & \frac{1}{8} (|1, 1, 3, 3\rangle - |1, 1, 4, 4\rangle - |1, 2, 2, 1\rangle - |1, 2, 3, 4\rangle - |1, 2, 4, 3\rangle - |1, 3, 1, 3\rangle - |1, 3, 3, 1\rangle - |1, 3, 4, 2\rangle \\ & - |1, 4, 1, 4\rangle - |2, 1, 2, 1\rangle - |2, 2, 1, 1\rangle - |2, 2, 4, 4\rangle - |2, 3, 1, 4\rangle - |2, 3, 3, 2\rangle - |2, 3, 4, 1\rangle - |2, 4, 1, 3\rangle \\ & - |2, 4, 2, 4\rangle - |2, 4, 4, 2\rangle - |3, 1, 1, 3\rangle - |3, 1, 2, 4\rangle - |3, 1, 3, 1\rangle - |3, 2, 3, 2\rangle - |3, 3, 1, 1\rangle - |3, 3, 2, 2\rangle \\ & - |3, 3, 3, 3\rangle - |3, 3, 4, 4\rangle - |3, 4, 1, 2\rangle - |3, 4, 2, 1\rangle - |3, 4, 3, 4\rangle - |4, 1, 1, 4\rangle - |4, 1, 2, 3\rangle - |4, 1, 3, 2\rangle \\ & - |4, 2, 2, 4\rangle - |4, 2, 3, 1\rangle - |4, 2, 4, 2\rangle - |4, 3, 3, 4\rangle - |4, 4, 2, 2\rangle - |4, 4, 4, 4\rangle + |1, 1, 1, 1\rangle + |1, 1, 2, 2\rangle \\ & + |1, 2, 1, 2\rangle + |1, 3, 2, 4\rangle + |1, 4, 2, 3\rangle + |1, 4, 3, 2\rangle + |1, 4, 4, 1\rangle + |2, 1, 1, 2\rangle + |2, 1, 3, 4\rangle + |2, 1, 4, 3\rangle \\ & + |2, 2, 2, 2\rangle + |2, 2, 3, 3\rangle + |2, 3, 2, 3\rangle + |2, 4, 3, 1\rangle + |3, 1, 4, 2\rangle + |3, 2, 1, 4\rangle + |3, 2, 2, 3\rangle + |3, 2, 4, 1\rangle \\ & + |3, 4, 4, 3\rangle + |4, 1, 4, 1\rangle + |4, 2, 1, 3\rangle + |4, 3, 1, 2\rangle + |4, 3, 2, 1\rangle + |4, 3, 4, 3\rangle + |4, 4, 1, 1\rangle + |4, 4, 3, 3\rangle) \end{aligned} \quad (\text{C1})$$

$$\begin{aligned} |O_{16}^{\text{alg}}\rangle = & (-0.0010 + 0.1768i) |3, 3, 3, 4\rangle + (0.1766 - 0.0079i) |2, 4, 3, 4\rangle + (-0.0091 + 0.1765i) |2, 4, 4, 2\rangle \\ & + (-0.1760 - 0.0163i) |3, 1, 3, 3\rangle + (0.0180 - 0.1759i) |4, 2, 1, 1\rangle + (0.1759 + 0.0180i) |3, 3, 4, 2\rangle \\ & + (0.2478 - 0.0328i) |2, 3, 1, 3\rangle + (-0.0338 + 0.1735i) |4, 4, 3, 3\rangle + (-0.2472 - 0.0373i) |3, 4, 2, 1\rangle \\ & + (0.1711 + 0.0443i) |1, 4, 4, 3\rangle + (-0.0483 + 0.1701i) |2, 1, 2, 2\rangle + (0.0627 + 0.1653i) |4, 2, 2, 3\rangle \\ & + (-0.2415 - 0.0645i) |1, 2, 3, 2\rangle + (-0.0654 + 0.1642i) |2, 1, 3, 1\rangle + (0.0675 - 0.1634i) |1, 3, 2, 4\rangle \\ & + (-0.1628 + 0.0690i) |2, 2, 4, 1\rangle + (-0.1613 + 0.0724i) |3, 2, 1, 4\rangle + (-0.1609 - 0.0732i) |4, 3, 2, 2\rangle \\ & + (0.0776 - 0.1588i) |3, 1, 1, 2\rangle + (-0.1569 - 0.0814i) |1, 1, 2, 3\rangle + (-0.0875 + 0.2342i) |4, 1, 4, 4\rangle \end{aligned}$$

$$\begin{aligned}
& + (0.0876 - 0.1535i) |1, 4, 1, 4\rangle + (0.1526 + 0.0893i) |4, 3, 3, 1\rangle + (0.1503 + 0.0931i) |4, 4, 1, 2\rangle \\
& + (-0.0984 + 0.1469i) |1, 3, 4, 1\rangle + (-0.1459 + 0.0998i) |2, 2, 2, 4\rangle + (-0.1039 - 0.1430i) |1, 1, 1, 1\rangle \\
& + (0.1122 + 0.1366i) |3, 2, 4, 3\rangle
\end{aligned} \tag{C2}$$

$$\begin{aligned}
|O_{16}^{\text{ref}}\rangle = & \frac{1}{4} \left(|1, 1, 1, 1\rangle + |2, 2, 2, 2\rangle + |3, 3, 3, 3\rangle + |4, 4, 4, 4\rangle + \frac{1}{\sqrt{2}} |1, 2, 3, 4\rangle - \frac{1}{\sqrt{2}} |1, 3, 2, 4\rangle - \frac{1}{\sqrt{2}} |2, 3, 4, 1\rangle \right. \\
& - \frac{1}{\sqrt{2}} |2, 4, 1, 3\rangle - \frac{1}{\sqrt{2}} |4, 2, 3, 1\rangle - \frac{1}{\sqrt{2}} |4, 3, 1, 2\rangle - \frac{i}{\sqrt{2}} |1, 4, 2, 3\rangle - \frac{i}{\sqrt{2}} |2, 1, 3, 4\rangle - \frac{i}{\sqrt{2}} |2, 3, 1, 4\rangle \\
& - \frac{i}{\sqrt{2}} |3, 2, 1, 4\rangle + \frac{i}{\sqrt{2}} |1, 2, 4, 3\rangle + \frac{i}{\sqrt{2}} |1, 4, 3, 2\rangle + \frac{i}{\sqrt{2}} |2, 4, 3, 1\rangle + \frac{i}{\sqrt{2}} |4, 2, 1, 3\rangle + \frac{1}{\sqrt{2}} |1, 3, 4, 2\rangle \\
& + \frac{1}{\sqrt{2}} |2, 1, 4, 3\rangle + \frac{1}{\sqrt{2}} |3, 1, 2, 4\rangle + \frac{1}{\sqrt{2}} |3, 1, 4, 2\rangle + \frac{1}{\sqrt{2}} |3, 2, 4, 1\rangle + \frac{1}{\sqrt{2}} |3, 4, 1, 2\rangle + \frac{1}{\sqrt{2}} |3, 4, 2, 1\rangle \\
& \left. + \frac{1}{\sqrt{2}} |4, 1, 2, 3\rangle + \frac{1}{\sqrt{2}} |4, 1, 3, 2\rangle + \frac{1}{\sqrt{2}} |4, 3, 2, 1\rangle \right).
\end{aligned} \tag{C3}$$

This example illustrates a case where the state obtained after applying the algorithm has reduced support, yielding a sparser representation. Specifically, the support of the original state is 64, whereas the support of the optimized state $|O_{16}^{\text{alg}}\rangle$ is 28.

Appendix D: Examples of optimal representations of AME states

In this section, we present additional examples demonstrating how the algorithm can be used to obtain simpler

and sparser representations of AME states. In particular, the cases of AME(4, 6), AME(5, 2), and AME(6, 2) are considered. It is known that only a single LU-equivalence class of AME(6, 2) states exists [80]. Although an infinite number of AME(5, 2) states exist [81], they all lie within a single two-dimensional subspace, and every AME(5, 2) state is LU-equivalent to an element of this subspace [80]. In all of these cases, the corresponding AME states are genuinely quantum. The examples are shown in Figs. 7–9, and the original states together with the local unitary matrices that map them to their final forms are provided in [73].

-
- [1] W. Dür, G. Vidal, and J. I. Cirac, *Physical Review A* **62**, 062314 (2000).
 - [2] M. Enríquez, Z. Puchała, and K. Życzkowski, *Entropy* **17**, 5063 (2015).
 - [3] W. Helwig, W. Cui, J. I. Latorre, A. Riera, and H.-K. Lo, *Physical Review A* **86**, 052335 (2012).
 - [4] A. Bernal Serrano, *Articles publicats en revistes (Matemàtiques i Informàtica)* (2017).
 - [5] W. Helwig and W. Cui, *Absolutely Maximally Entangled States: Existence and Applications* (2013), arXiv:1306.2536 [quant-ph].
 - [6] A. J. Scott, *Physical Review A* **69**, 052330 (2004).
 - [7] Z. Raissi, C. Gogolin, A. Riera, and A. Acín, *Journal of Physics A: Mathematical and Theoretical* **51**, 075301 (2018).
 - [8] D. Alsina and M. Razavi, *Physical Review A* **103**, 022402 (2021).
 - [9] F. Huber and M. Grassl, *Quantum* **4**, 284 (2020).
 - [10] F. Pastawski, B. Yoshida, D. Harlow, and J. Preskill, *Journal of High Energy Physics* **2015**, 149 (2015).
 - [11] F. Pastawski and J. Preskill, *Physical Review X* **7**, 021022 (2017).
 - [12] T. J. Osborne and D. E. Stiegemann, *Journal of High Energy Physics* **2020**, 154 (2020).
 - [13] P. Mazurek, M. Farkas, A. Grudka, M. Horodecki, and M. Studziński, *Physical Review A* **101**, 042305 (2020).
 - [14] A. Jahn and J. Eisert, *Quantum Science and Technology* **6**, 033002 (2021).
 - [15] M. Steinberg, S. Feld, and A. Jahn, *Nature Communications* **14**, 7314 (2023).
 - [16] R. Bistoń, M. Hontarenko, and K. Życzkowski, *Physical Review D* **111**, 026006 (2025).
 - [17] Open Quantum Problems – Open Quantum Problems : <https://oqp.iqoqi.oeaw.ac.at/open-quantum-problems>.
 - [18] A. Higuchi and A. Sudbery, *Physics Letters A* **273**, 213 (2000).
 - [19] C. H. Bennett, D. P. DiVincenzo, J. A. Smolin, and W. K. Wootters, *Physical Review A* **54**, 3824 (1996).
 - [20] F. Huber, O. Gühne, and J. Siewert, *Physical Review Letters* **118**, 200502 (2017).
 - [21] F. Huber and N. Wyderka, *Table of AME states / perfect tensors*, <https://tp.nt.uni-siegen.de/ame/ame.html>.
 - [22] M. Hein, J. Eisert, and H. J. Briegel, *Physical Review A* **69**, 062311 (2004).
 - [23] W. Helwig, *Absolutely Maximally Entangled Qudit Graph States* (2013), arXiv:1306.2879 [quant-ph].
 - [24] M. Grassl, T. Beth, and M. Rötteler, *International Journal of Quantum Information* **02**, 55 (2004).
 - [25] D. Goyeneche, D. Alsina, J. I. Latorre, A. Riera, and K. Życzkowski, *Physical Review A* **92**, 032316 (2015).
 - [26] D. Goyeneche, Z. Raissi, S. Di Martino, and K. Życzkowski, *Physical Review A* **97**, 062326 (2018).

- arXiv:1708.05946 [quant-ph].
- [27] L. Clarisse, S. Ghosh, S. Severini, and A. Sudbery, *Physical Review A* **72**, 012314 (2005).
- [28] C. H. Bennett, H. J. Bernstein, S. Popescu, and B. Schumacher, *Physical Review A* **53**, 2046 (1996).
- [29] C. H. Bennett, S. Popescu, D. Rohrlich, J. A. Smolin, and A. V. Thapliyal, *Physical Review A* **63**, 012307 (2000).
- [30] A. Acín, A. Andrianov, L. Costa, E. Jané, J. I. Latorre, and R. Tarrach, *Physical Review Letters* **85**, 1560 (2000).
- [31] A. Burchardt and Z. Raissi, *Physical Review A* **102**, 022413 (2020).
- [32] Y. Liu, P. Sierant, P. Stornati, M. Lewenstein, and M. Płodzień, *Physical Review A* **111**, 052614 (2025).
- [33] S. A. Rather, A. Burchardt, W. Bruzda, G. Rajchel-Mieldzióć, A. Lakshminarayan, and K. Życzkowski, *Physical Review Letters* **128**, 080507 (2022).
- [34] K. Życzkowski, W. Bruzda, G. Rajchel-Mieldzióć, A. Burchardt, S. A. Rather, and A. Lakshminarayan, *Journal of Physics: Conference Series* **2448**, 012003 (2023).
- [35] G. Tarry, *Secrétariat de l'Association française pour l'avancement des sciences* (1900).
- [36] S. A. Rather, N. Ramadas, V. Kodiyalam, and A. Lakshminarayan, *Physical Review A* **108**, 032412 (2023).
- [37] S. A. Rather, *Quantum* **8**, 1528 (2024).
- [38] W. Bruzda and K. Życzkowski, *Special Matrices* **12**, 10.1515/spma-2024-0010 (2024).
- [39] D. Gross and P. Goedicke, *Thirty-six officers, artisanally entangled* (2025), arXiv:2504.15401 [quant-ph].
- [40] M. Enríquez, I. Wintrowicz, and K. Życzkowski, *Journal of Physics: Conference Series* **698**, 012003 (2016).
- [41] K. Chen and L.-A. Wu, *Quantum Information and Computation* **3**, 193 (2003).
- [42] A. Peres, *Physical Review Letters* **77**, 1413 (1996).
- [43] B. Musto and J. Vicary, *Quantum Information and Computation* **16**, 1318 (2016).
- [44] H. A. Carteret, A. Higuchi, and A. Sudbery, *Journal of Mathematical Physics* **41**, 7932 (2000), arXiv:quant-ph/0006125.
- [45] S. Bravyi, *Physical Review A* **67**, 012313 (2003).
- [46] T.-C. Wei and P. M. Goldbart, *Physical Review A* **68**, 042307 (2003).
- [47] D. Thouless, *Physics Reports* **13**, 93 (1974).
- [48] B. Kramer and A. MacKinnon, *Reports on Progress in Physics* **56**, 1469 (1993).
- [49] F. Evers and A. D. Mirlin, *Rev. Mod. Phys.* **80**, 1355 (2008).
- [50] A. Rodriguez, L. J. Vasquez, and R. A. Römer, *Phys. Rev. Lett.* **102**, 106406 (2009).
- [51] A. Rodriguez, L. J. Vasquez, K. Slevin, and R. A. Römer, *Phys. Rev. Lett.* **105**, 046403 (2010).
- [52] T. C. Halsey, M. H. Jensen, L. P. Kadanoff, I. Procaccia, and B. I. Shraiman, *Physical review A* **33**, 1141 (1986).
- [53] H. E. Stanley and P. Meakin, *Nature* **335**, 405 (1988).
- [54] M. Dziurawiec, J. O. de Almeida, M. L. Bera, M. Płodzień, M. M. Maśka, M. Lewenstein, T. Grass, and U. Bhattacharya, *Phys. Rev. B* **110**, 014209 (2024).
- [55] I. García-Mata, O. Giraud, and B. Georgeot, *Phys. Rev. A* **79**, 052321 (2009).
- [56] A. Bäcker, M. Haque, and I. M. Khaymovich, *Phys. Rev. E* **100**, 032117 (2019).
- [57] J.-M. Stéphan, S. Furukawa, G. Misguich, and V. Pasquier, *Phys. Rev. B* **80**, 184421 (2009).
- [58] J.-M. Stéphan, G. Misguich, and V. Pasquier, *Phys. Rev. B* **82**, 125455 (2010).
- [59] J.-M. Stéphan, *Phys. Rev. B* **90**, 045424 (2014).
- [60] D. J. Luitz, F. Alet, and N. Laflorencie, *Phys. Rev. Lett.* **112**, 057203 (2014).
- [61] D. J. Luitz, X. Plat, N. Laflorencie, and F. Alet, *Phys. Rev. B* **90**, 125105 (2014).
- [62] M. Pino, V. E. Kravtsov, B. L. Altshuler, and L. B. Ioffe, *Phys. Rev. B* **96**, 214205 (2017).
- [63] J. Lindinger, A. Buchleitner, and A. Rodríguez, *Phys. Rev. Lett.* **122**, 106603 (2019).
- [64] L. Pausch, E. G. Carnio, A. Rodríguez, and A. Buchleitner, *Phys. Rev. Lett.* **126**, 150601 (2021).
- [65] P. Frey, D. Mikhail, S. Rachel, and L. Hackl, *Phys. Rev. B* **109**, 064302 (2024).
- [66] F. S. Lozano-Negro, P. R. Zangara, and H. M. Pastawski, *Chaos, Solitons & Fractals* **150**, 111175 (2021).
- [67] A. De Luca and A. Scardicchio, *EPL (Europhysics Letters)* **101**, 37003 (2013).
- [68] P. Sierant and X. Turkeshi, *Physical Review Letters* **128**, 130605 (2022).
- [69] P. Sierant, M. Schirò, M. Lewenstein, and X. Turkeshi, *Phys. Rev. B* **106**, 214316 (2022).
- [70] S. A. Rather, S. Aravinda, and A. Lakshminarayan, *Construction and local equivalence of dual-unitary operators: From dynamical maps to quantum combinatorial designs* (2022), arXiv:2205.08842 [cond-mat, physics:math-ph, physics:nlin, physics:quant-ph].
- [71] N. Kwak, *IEEE Transactions on Cybernetics* **44**, 594 (2014).
- [72] J. Steinberg and O. Gühne, *Physical Review A* **110**, 062428 (2024).
- [73] N. Ramadas, *Minimal decomposition entropy*, <https://github.com/lzwez/minimal-decomposition-entropy>.
- [74] A. Streltsov, H. Kampermann, and D. Bruß, *Physical Review A* **84**, 022323 (2011).
- [75] L. T. Weinbrenner and O. Gühne, *Europhysics Letters* **151**, 68001 (2025).
- [76] D. Goyeneche and K. Życzkowski, *Physical Review A* **90**, 022316 (2014).
- [77] S. A. Rather, S. Aravinda, and A. Lakshminarayan, *Physical Review Letters* **125**, 070501 (2020).
- [78] P. H. Schönemann, *Psychometrika* **31**, 1 (1966).
- [79] A. Sayed, *Foundations and Trends® in Machine Learning* **7**, 311 (2014).
- [80] E. Rains, *IEEE Transactions on Information Theory* **45**, 266 (1999).
- [81] N. Ramadas and A. Lakshminarayan, *Journal of Physics A: Mathematical and Theoretical* **58**, 125301 (2025).